UNIVERSITY of York

This is a repository copy of *Thermodynamics of interacting magnetic nanoparticles*.

White Rose Research Online URL for this paper:
https://eprints.whiterose.ac.uk/168248/

Version: Accepted Version

Article:
Torche, P., Munoz-Menendez, C., Serantes, D. et al. (6 more authors) (2020) Thermodynamics of interacting magnetic nanoparticles. Physical Review B. 224429. ISSN 2469-9969

https://doi.org/10.1103/PhysRevB.101.224429

Reuse
Items deposited in White Rose Research Online are protected by copyright, with all rights reserved unless indicated otherwise. They may be downloaded and/or printed for private study, or other acts as permitted by national copyright laws. The publisher or other rights holders may allow further reproduction and re-use of the full text version. This is indicated by the licence information on the White Rose Research Online record for the item.

Takedown
If you consider content in White Rose Research Online to be in breach of UK law, please notify us by emailing eprints@whiterose.ac.uk including the URL of the record and the reason for the withdrawal request.

White Rose university consortium
Universities of Leeds, Sheffield & York

eprints@whiterose.ac.uk
https://eprints.whiterose.ac.uk/

Thermodynamics of interacting magnetic nanoparticles

P. Torche[1], C. Munoz-Menendez[2], D. Serantes[2], D. Baldomir[2], K. L. Livesey[3], O. Chubykalo-Fesenko[4], S. Ruta[5], R. Chantrell[5], and O. Hovorka[1*]

[1] *School of Engineering and Physical Sciences, University of Southampton, Southampton SO16 7QF, UK*

[2] *Instituto de Investigacións Tecnolóxicas and Departamento de Física Aplicada, Universidade de Santiago de Compostela, 15782 Santiago de Compostela, Spain*

[3] *UCCS Biofrontiers Center and Department of Physics, University of Colorado at Colorado Springs, Colorado Springs, Colorado 80918, USA*

[4] *Instituto de Ciencia de Materiales de Madrid, CSIC, Cantoblanco, ES-28049 Madrid, Spain and*

[5] *Department of Physics, University of York, York YO10 5DD, UK*

(Dated: June 5, 2020)

We apply the concepts of stochastic thermodynamics combined with the transition state theory to develop a framework for evaluating local heat distributions across the assemblies of interacting magnetic nanoparticles (MP) subject to time-varying external magnetic fields. We show that additivity of entropy production in the particle state-space allows separating the entropy contributions and evaluating the heat produced by the individual MPs despite interactions. Using MP chains as a model system for convenience, without losing generality, we show that the presence of dipolar interactions leads to significant heat distributions across the chains. Our study also suggests that the typically used hysteresis loops cannot be used as a measure of energy dissipation at the local particle level within MP clusters, aggregates or assemblies, and explicit evaluation of entropy production based on appropriate theory, such as developed here, becomes necessary.

I. INTRODUCTION

Magnetic nanoparticles (MP) are prototypical examples of out-of-equilibrium thermodynamic systems. Their behaviour is often manifested by memory effects and hysteresis, which are exploited in a variety of applications ranging from information storage to environmentally friendly refrigeration and medicine [1–5]. A fully consistent non-equilibrium thermodynamics of MPs that would allow advancing these applications still remains to be developed, especially for systems with non-negligible inter-particle interactions.

For example, the complementary approach to cancer therapy based on MP hyperthermia, where MPs internalised inside cancerous cells and subject to alternating magnetic fields heat the tumours to cytotoxic temperatures, requires relating the heat production to physical properties of MPs and time varying fields [6]. It also requires understanding the effects of inter-particle interactions, which become significant when MPs aggregate during the internalisation inside cells and most frequently lead to the reduction of the heating efficiency [7–9]. Moreover, it is currently unclear if it is the net heating effect of the entire MP aggregate or the local heat distribution across it that leads to tumour death [10–14]. Answering these questions, and analogous questions pertaining to other applications, requires developing a consistent non-equilibrium thermodynamic description of systems of interacting MPs.

The challenge is that due to the small size of MPs, thermal fluctuations become dominant and applying the standard non-equilibrium thermodynamics founded on the assumption of 'local equilibrium' becomes problematic [15]. Similarly, the frequently used linear response theory is limited only to dynamical processes close to equilibrium [16, 17]. Thermodynamics of hysteresis based on superimposed collections of bistable elements [18, 19], or the more general stochastic approach to non-equilibrium thermodynamics [20–22] were also proposed, but so far remain unused for systematic studies of systems of interacting MPs.

In this work we fill the gap and apply the non-equilibrium stochastic thermodynamics combined with the standard transition state theory [21, 22] to systems of interacting MPs. We show that it is possible to associate the expressions for entropy production with the individual MPs within an interacting assembly, which in turn allows computing the single particle heat distribution across the assembly. Although the formalism is general, to simplify the computations we consider chains of identical MPs with aligned uniaxial anisotropy and coupled by dipolar interactions. This configuration allows obtaining analytical expressions for the energy barriers and thermal transitions rates, and applying the Markovian probabilistic master-equation formalism frequently employed for modelling the long-timescale thermal fluctuations in MP systems.

Solving numerically the full master-equation we quantify the temporal evolution of the particle states, and through the developed thermodynamics formalism evaluate the individual particle heat inside the chains. Our calculations suggests that dipolar interactions lead to significant heat distribution across chains, often varying by as much as 50% - 100% of the mean heat practically measurable from the hysteresis loop area of an entire MP system, which is a significant finding. We also show that due to the presence of interactions, the area of the hysteresis

* o.hovorka@soton.ac.uk

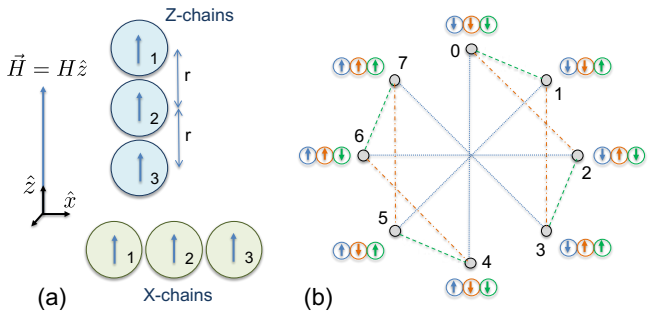

FIG. 1. (a) Illustration of chains of $N = 3$ particles in 'Z' configuration such that $\hat{r}_{ij} \parallel \hat{k} \parallel \vec{H}$, and in 'X' configuration with $\hat{r}_{ij} \perp \hat{k} \parallel \vec{H}$. Inter-particle distance is denoted by r, and $\vec{H}$ is the applied field vector. (b) A sketch of a network of possible single-particle transitions between the 2^3 states α of a 3-particle chain. Dashed, dash-dotted, and dotted lines correspond to transitions of the right, middle, and left particle.

sub-loops corresponding to the individual MPs does not represent the particle heat, and performing explicit calculations based on evaluating the entropy production is necessary.

The article is organised as follows. Section II introduces the model of interacting MPs including the thermally activated dynamics described by the standard transition state theory. Thermodynamics of particle chains is discussed in Section III, based on the definitions of the first law of thermodynamics and entropy balance. Section IV offers similar discussion related to thermodynamics of individual particles within a chain. Thermodynamic implications of the practically relevant cyclic processes produced by alternating external magnetic fields are discussed in Section V. The discussion of the dipolar effects and conclusions are given in Sections VI and VII.

II. MODEL OF THERMALLY ACTIVATED PARTICLE CHAINS

To use a specific well established model of MPs, we consider chains of N interacting identical particles, each having diameter a, volume V, and uniaxial anisotropy $\vec{K} = K\hat{k}$ oriented along the $\hat{z}$ axis of the coordinate system (Fig. 1). The standard form of the energy per particle volume of the chain reads [23]:

$$\frac{E}{V} = \sum_i \left(-K(\hat{k} \cdot \hat{s}_i)^2 - \mu_0 M_s \hat{s}_i \cdot \left(\vec{H} + \vec{H}_i^{\rm d} \right) \right) \qquad (1)$$

where the first term in the sum is the unaxial anisotropy energy of particles i and the second term quantifies the interaction between the particles and the applied and dipolar magnetic fields, $\vec{H}$ and $\vec{H}_i^{\rm d}$, respectively. The dipolar field $\vec{H}_i^{\rm d}$ is produced by all neighbouring particles of a particle i in the chain, and is given by the standard expression:

$$\vec{H}_i^{\rm d} = -\frac{M_s V}{4\pi a^3} \sum_{j<i} \frac{1}{r_{ij}^3} \left(-\hat{s}_j + 3(\hat{s}_j \cdot \hat{r}_{ij})\hat{r}_{ij} \right) \qquad (2)$$

where $r_{ij} = R_{ij}/a$ corresponds to particle-to-particle distances normalised by the particle diameter a. The distance between the neighbouring particles will be denoted by the symbol r. The dimensionless particle moment vectors $\hat{s}_i$ follow from the definition of an intrinsic magnetic moment of a MP:

$$\vec{m}_i = V M_s \hat{s}_i \qquad (3)$$

where M_s is the saturation magnetisation.

The minima of energy Eq. (1) correspond to stable spin configurations defining the states α of the system. Thermally activated dynamics is described by the transition state theory as a hopping process between the states, with transition rates from any state β to α determined by the standard Arrhenius form [24]:

$$w_{\alpha\beta} = f_0 \exp\left(-\frac{\Delta E_{\alpha\beta}}{k_B T} \right) \qquad (4)$$

where $\Delta E_{\alpha\beta}$ are the energy barriers separating the states α and β, the constant f_0 is the attempt frequency, k_B is the Boltzmann constant, and T is temperature. Finding the energy barriers in many-particle systems is generally a difficult optimisation problem. Here we restrict our considerations to co-linear particle chains and assume single-particle transitions, as illustrated in Fig. 1, which allows expressing the energy barriers analytically as [25]:

$$\Delta E_{\alpha\beta} = KV \left(1 \pm \frac{|\vec{H} + \vec{H}_i^{\rm d}|}{H_K} \right)^2 \qquad (5)$$

where the dipolar field index i implies that the states α and β are related by the switched particle i (Fig. 1(b)), and $H_K = 2K/\mu_0 M_s$. The '$\pm$' sign in Eq. (5) refers to energy barriers for particle i switching down $(+)$ or up $(-)$, respectively. Detailed discussion of the algorithms used to track down the network of single particle transitions and computing the energy barriers in more general cases of non-colinear particles was presented earlier [26, 27]. The assumption of single particle transitions is valid for weakly interacting systems with the negligible likelihood of correlated switching events, which according to Eq. (2) is be expected roughly when $NM_S V/4\pi a^3 << H_K$.

The time evolution of state probabilities $P_\alpha(t)$ is prescribed by a master equation [24, 28]:

$$\frac{dP_\alpha(t)}{dt} = \sum_\beta \left(w_{\alpha\beta}(t) P_\beta(t) - w_{\beta\alpha}(t) P_\alpha(t) \right) \qquad (6)$$

solving which allows specifying the time-dependent probability distribution for all states α, which fully characterises the time evolution of the system. From the mathematical point of view, Eq. (6) is a set of 1-st order

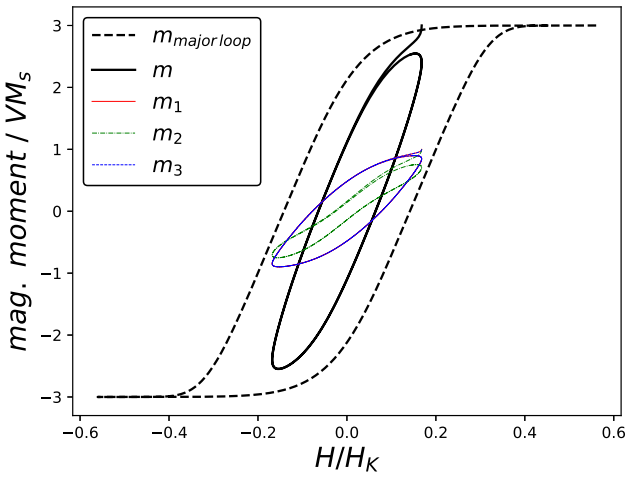

FIG. 2. Hysteresis loops corresponding to a 3-particle chain configuration X illustrated in Fig. 1. The thick dashed and solid line loops were computed upon subjecting the chain to field amplitudes $H_0 = 80$ kA/m and 24 kA/m, respectively. The thin lines m_i with $i = 1, 2, 3$ show the cycles corresponding to individual particles in the chain assuming $H_0 = 24$ kA/m. The simulation parameters were as described in the text, with $a = 11$ nm, $r = 1.2a$, and $f = 300$ kHz.

ordinary differential equations subject to the initial condition $P_\alpha(0)$ for all α.

The transition network in simulations presented below was set up by tracking the single-particle state differences using the algorithm discussed earlier [26, 27]. This allowed to construct Eq. (6), which was then solved by the standard ODE integrators based on explicit Runge-Kutta methods [29]. The chosen initial condition $P_\alpha(0)$ corresponded to a large positive field value, which guaranteed the initial state α^* with all MPs pointing along the field direction, i.e. $P_\alpha(0) = 1$ for $\alpha = \alpha^*$ and $P_\alpha(0) = 0$ for $\alpha \neq \alpha^*$. Since the number of states entering in these simulations grows as 2^N, the computational complexity grows accordingly allowing one to treat only relatively short chains of a few tens of MPs.

The simulation parameters were chosen to represent Fe_3O_4 particles often considered for medical applications due to their biocompatibility. The uniaxial anisotropy in Eq. (1) was set to $K = 4 \times 10^4$ J/m^3, and the saturation magnetisation was $M_s = 446$ kA/m. A periodic applied magnetic field was assumed as $\vec{H} = H_0 \cos(2\pi f t)\hat{z}$ with amplitude H_0 and frequency f. The temperature and attempt frequency entering in Eq. (4) were set to $T = 300$ K and $f_0 = 10^9$ s^{-1}. We studied particle chains of length up to $N = 10$ particles.

Fig. 2 shows examples of hysteresis loops computed for the 3-particle X chain illustrated in Fig. 1. The dashed and thick solid lines show, respectively, the major and minor hysteresis cycles corresponding to the field amplitudes $H_0 = 80$ kA/m and $H_0 = 24$ kA/m. The plotted total thermal magnetic moment $\vec{m}$ was calculated by averaging Eq. (3) over all particles as:

$$\vec{m}(t) = VM_s \sum_\alpha \sum_i \hat{s}_i^\alpha P_\alpha(t) \tag{7}$$

where $\hat{s}_i^\alpha$ denote the spin configurations corresponding to the stable states α obtained as minima of Eq. (1), and $P_\alpha(t)$ are the solutions of Eq. (6).

Similarly, the magnetic moments of individual particles $\vec{m}_i$ in the chain shown by the sub-loops in Fig. 2 were computed as:

$$\vec{m}_i(t) = VM_s \sum_\alpha \hat{s}_i^\alpha P_\alpha(t) \tag{8}$$

Eq. (8) was obtained from Eq. (7) after exchanging the order of the sums and expressing $\vec{m}(t) = \sum_i \vec{m}_i(t)$. Due to the symmetry of the chain the sub-loops corresponding to the side particles ($i = 1$ and 3) are identical, while the sub-loop of the central particle is qualitatively distinguished as a result of a different dipolar field in the centre of the chain. The three sub-loops add up to form the chain's minor hysteresis cycle shown by the thick solid line. Note also that due to thermal activation, the hysteresis loops are frequency dependent. For slow frequencies the system recovers the superparamagnetic regime with any hysteresis effects absent, as expected.

It is worth pointing out that the thermally activated dynamics of MPs considered here, sometimes termed as the Néel-Brown theory or the discrete orientation model [24], is in the limit of high energy barriers and high damping fully consistent with the Langevin dynamics approach based on the stochastic Landau-Lifshitz-Gilbert equation [24, 30, 31]. The present master-equation approach has been subject to successful experimental validations [32–34], and is the method of choice for studying the long-time-scale thermally activated dynamics when the Langevin framework becomes computationally inefficient.

Finally, note that the vector notation used in the formulas above is not necessary, as the magnetic moments of MPs in the assumed aligned chain configurations (Fig. 1) are always aligned either along or against the external magnetic field direction. However, the presented framework can be applied to arbitrary particle configuration [26, 27], assuming the corresponding energy barriers can be identified either analytically or numerically. For this reason we use the vector form in the expressions when relevant.

III. THERMODYNAMICS OF A PARTICLE SYSTEM

The first law of thermodynamics for magnetic systems can be expressed as:

$$\frac{dU}{dt} = \frac{\delta W}{\delta t} + \frac{\delta Q^e}{\delta t} \tag{9}$$

stating that the rate of change of the internal system energy U depends on the incremental magnetic work performed on the particle system by the external magnetic fields and on the heat exchanged between the system and the heat bath. The differential notation 'δ' is used to distinguish process-dependent variables such as work W or heat Q^e, and state variables such as the internal energy U quantifiable by the total differentials and dependent only on the starting and ending states visited during the system evolution.

The magnetic work is typically presented in one of the following forms:

$$\frac{\delta W}{\delta t} = -\mu_0 \vec{m} \cdot \frac{d\vec{H}}{dt} \tag{10}$$

or:

$$\frac{\delta W}{\delta t} = \mu_0 \vec{H} \cdot \frac{d\vec{m}}{dt} \tag{11}$$

The difference between $U(H)$ and $U(M)$ with work expressions given, respectively, by Eqs. (10) and (11) is that whereas $U(M)$ includes the energy stored in the applied field, it is excluded from $U(H)$ [35]. However, since both representations are related by Legendre transformation $U(H) = U(M) - \mu_0 \vec{m} \cdot \vec{H}$, the thermodynamic consequences of either formulation are identical. We will base our definition of magnetic work on Eq. (10), which is typically the form used in statistical mechanics for describing systems prescribed by effective hamiltonians [36].

The internal system energy U entering in Eq. (9) is postulated as weighted average [21]:

$$U(t) = \sum_{\alpha} E_\alpha(t) P_\alpha(t) \tag{12}$$

where E_α are the state energies corresponding to the minima of Eq. (1). The probabilities $P_\alpha(t)$ are obtained by solving Eq. (6) and prescribe the thermally activated changes in the density of populations of states α. It is straightforward to check that after setting the time derivative in Eq. (6) to zero and using the resulting detailed balance condition, Eq. (12) reduces to $U = \sum_\alpha E_\alpha P_\alpha^{eq}$, where the thermal equilibrium state probabilities $P_\alpha^{eq} = \lim_{t\to\infty} P_\alpha(t) \propto \exp\left(-E_\alpha/k_B T\right)$ are consistent with Boltzmann distribution, as expected.

The heat exchange term Q^e entering in Eqs. (9) can be related to the entropy flow between the particle system and the environment by using the Carnot-Clausius theorem [15]:

$$\frac{\delta Q^e}{\delta t} = T \frac{\delta_e S}{\delta t} \tag{13}$$

which is valid for closed systems able to exchange only the heat with the environment, such as considered in this study. Inserting Eq. (10) and (13) in Eq. (9) we obtain:

$$\frac{dU}{dt} = -\mu_0 \vec{m} \cdot \frac{d\vec{H}}{dt} + T \frac{\delta_e S}{\delta t} \tag{14}$$

which is the form of the first thermodynamic law used further.

It turns out there is a close relationship between the entropy flow and the structure of the Master equation Eq. (6), which can be revealed as follows. The Gibbs non-equilibrium entropy takes the standard form [20, 21]:

$$S(t) = -k_B \sum_{\alpha} P_\alpha(t) \ln P_\alpha(t) \tag{15}$$

The rate of change of entropy is split into entropy flow $\delta_e S/\delta t$ and entropy production $\delta_p S/\delta t$ [15]:

$$\frac{dS}{dt} = \frac{\delta_e S}{\delta t} + \frac{\delta_p S}{\delta t} \tag{16}$$

The explicit expressions for the entropy contributions in Eq. (16) can be obtained by inserting Eq. (6) into the differentiated total entropy Eq. (15) and arranging, which leads to:

$$\frac{dS}{dt} = \frac{k_B}{2} \sum_{\alpha\beta} \left(w_{\alpha\beta} P_\beta - w_{\beta\alpha} P_\alpha\right) \ln \frac{P_\beta}{P_\alpha} \tag{17}$$

and:

$$\frac{\delta_p S}{\delta t} = \frac{k_B}{2} \sum_{\alpha\beta} \left(w_{\alpha\beta} P_\beta - w_{\beta\alpha} P_\alpha\right) \ln \frac{w_{\alpha\beta} P_\beta}{w_{\beta\alpha} P_\alpha} \tag{18}$$

and:

$$\frac{\delta_e S}{\delta t} = -\frac{k_B}{2} \sum_{\alpha\beta} \left(w_{\alpha\beta} P_\beta - w_{\beta\alpha} P_\alpha\right) \ln \frac{w_{\alpha\beta}}{w_{\beta\alpha}} \tag{19}$$

Eq. (18) postulates the expression for entropy production quantifying the extent of irreversible processes occurring within a system [28], and hence Eq. (19) defines the entropy flow. The entropy flow $\delta_e S/\delta t$ can be positive or negative, depending on the interaction between the system and its surroundings, and relates to the amount of exchanged heat through Eq. (13). On the other hand, the second law of thermodynamics demands the entropy production to be non-negative [15]:

$$\frac{\delta_p S}{\delta t} \geq 0 \tag{20}$$

This condition holds for Eq. (18) naturally since the term in the natural logarithm is positive if $w_{\alpha\beta} P_\beta > w_{\beta\alpha} P_\alpha$, and it is negative if $w_{\alpha\beta} P_\beta < w_{\beta\alpha} P_\alpha$, which always balances the positive and negative signs in the overall expression. The equality sign $\delta_p S/\delta t = 0$ applies only for reversible (equilibrium) transformations.

Finally, the heat produced by the system can be defined analogously to Eq. (13) as:

$$\frac{\delta Q^p}{\delta t} = T \frac{\delta_p S}{\delta t} \tag{21}$$

Eq. (17)-(19) and (21) can be evaluated in a straightforward way after solving the master equation Eq. (6). Moreover, the definitions above are consistent with the first thermodynamics law (14) as can be confirmed through a straightforward algebraic exercise.

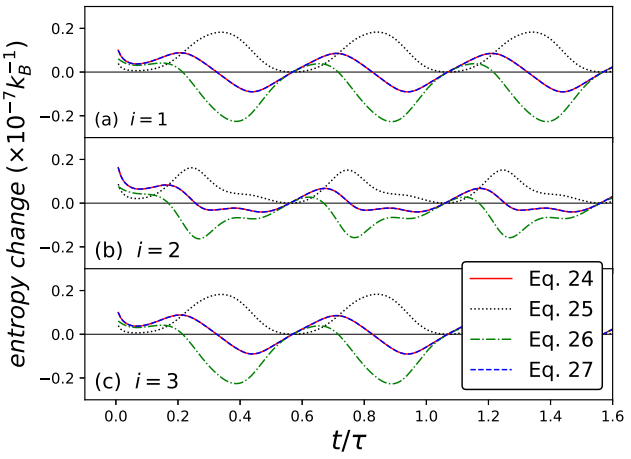

FIG. 3. Time dependence of the entropy change, entropy production, and entropy flow for individual particles $i = 1, 2, 3$ in the 3-particle X chain (Fig. 1). Particles $i = 1$ and 3 respond equally due to the symmetry of the chain. The simulation parameters were as described in the text, with $a = 11$ nm, $r = 1.2a$, $H_0 = 24$ kA/m, $f = 300$ kHz, and $\tau = 1/f$ being the field period.

IV. THERMODYNAMICS OF AN EMBEDDED PARTICLE

The key question is whether the first thermodynamic law equation defined by Eq. (14) can be reduced to apply separately to individual MP embedded in a chain. It turns out that in general this is not possible because the non-linearity in the dipolar interaction term in Eqs. (1) and (2) does not allow expressing the internal system energy Eq. (12) as a superposition of contributions from the individual MPs in a chain. However, as we show below, it is possible to associate the magnetic work and entropy with the individual MPs, and then quantify their heat production.

The magnetic work term in Eq. (14) can be expressed as a sum over the particles $\mu_0\vec{m}\cdot d\vec{H}/dt = \sum_i \mu_0\vec{m}_i \cdot d\vec{H}/dt$, where $\vec{m}_i$ is given by Eq. (8), from which the incremental work associated with the particle i in the system follows as:

$$\frac{\delta W_i}{\delta t} = -\mu_0\vec{m}_i \cdot \frac{d\vec{H}}{dt} \tag{22}$$

Eq. (22) can be evaluated independently for all MPs in a chain.

To express the entropy of a particle in the system, we first observe that Eqs. (17)-(19) are represented as sums of contributions from all available single particle transitions. This additive form allows to rewrite these equations as sums over the transitions corresponding to the switching events of individual particles (see Fig. 1(b)), and express Eq. (16) as:

$$\sum_i \frac{dS_i}{dt} = \sum_i \frac{\delta_e S_i}{\delta t} + \sum_i \frac{\delta_p S_i}{\delta t} \tag{23}$$

where the total entropy change of a particle reads:

$$\frac{dS_i}{dt} = \frac{k_B}{2}\sum_{\alpha\beta}^{i} (w_{\alpha\beta}P_\beta - w_{\beta\alpha}P_\alpha)\ln\frac{P_\beta}{P_\alpha} \tag{24}$$

the entropy production of a particle is:

$$\frac{\delta_p S_i}{\delta t} = \frac{k_B}{2}\sum_{\alpha\beta}^{i} (w_{\alpha\beta}P_\beta - w_{\beta\alpha}P_\alpha)\ln\frac{P_\beta w_{\alpha\beta}}{P_\alpha w_{\beta\alpha}} \tag{25}$$

and the particle entropy flow follows as:

$$\frac{\delta_e S_i}{\delta t} = -\frac{k_B}{2}\sum_{\alpha\beta}^{i} (w_{\alpha\beta}P_\beta - w_{\beta\alpha}P_\alpha)\ln\frac{w_{\alpha\beta}}{w_{\beta\alpha}} \tag{26}$$

The symbols $\sum^i$ in Eqs. (24)-(26) imply that the summation is to be carried out only over the pairs of states associated with transitions of a particle i (e.g. dashed, dotted, dash-dotted lines in Fig. 1(b)).

Eqs. (23)-(26) suggest the entropy balance for individual MPs:

$$\frac{dS_i}{dt} = \frac{\delta_e S_i}{\delta t} + \frac{\delta_p S_i}{\delta t} \tag{27}$$

analogous to Eq. (16). This hypothesis is plausible because the contributions from the individual transition paths summed over in Eqs. (24)-(26) are non-overlapping. It is also plausible to interpret $\delta_p S_i/\delta t$ as the single particle entropy production since applying the argumentation used to justify Eq. (20) leads again to the necessary condition:

$$\frac{\delta_p S_i}{\delta t} \geq 0 \tag{28}$$

We have performed extensive computations to validate Eqs. (27) and (28), such as shown Fig. 3 for the case of 3-particle chain in X configuration.

Finally, we associate the heat contributions with a particle i analogously to Eqs. (13) and (21) as:

$$\frac{\delta Q_i^e}{\delta t} = \frac{\delta_e S_i}{\delta t} \quad \text{and} \quad \frac{\delta Q_i^p}{\delta t} = \frac{\delta_p S_i}{\delta t} \tag{29}$$

which will be used in the following sections to study the heat distributions across chains of variable length.

V. CYCLIC PROCESSES

The formalism developed above allows evaluating magnetic and thermodynamic behaviour of particle systems subject to arbitrary external field variation. Practically relevant are, for instance, constant applied fields used in

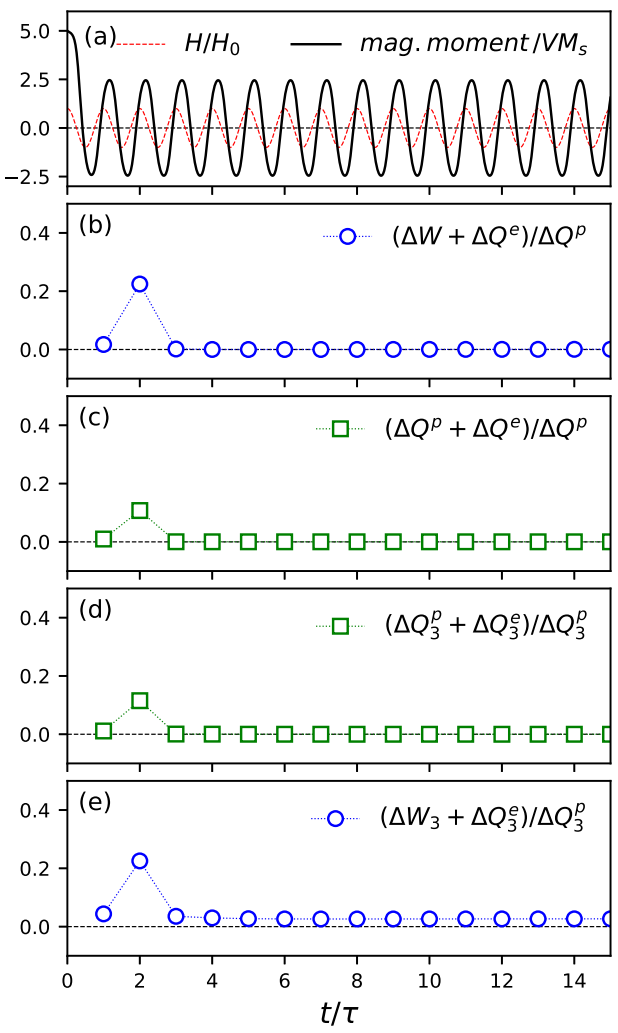

FIG. 4. Validation of thermodynamic relations for a 5-particle chain configuration X (Fig. 1), over several external field periods τ. (a) Time dependence of magnitudes of the magnetic field $\vec{H}$ and total magnetic moment $\vec{m}$ per VM_s. (b)-(e) validation of Eqs. (31), (33), (38), and (36) for particle $i = 3$ in the chain, respectively. Simulation parameters were: $a = 13$ nm, $H_0 = 24$ kA/m, $f = 300$ kHz, and $r = 1.2a$.

magnetorelaxometry [4, 27], pulsed fields used in magnetic resonance imaging, or periodic (cyclic) field variations used in magnetic particle imaging [5] and hyperthermia [6].

As an example, Fig. 4(a) shows the time dependence of the magnetic moment of a 5-particle X chain subject to periodic magnetic field. The figure shows that after the initial transient time, which can be short or long depending on the MP properties, the system evolution settles into a periodic steady state. To evaluate the amount of heat produced by MPs during the field cycle, Eq. (14) can be integrated and expressed as:

$$\Delta U = \Delta W + \Delta Q^e \tag{30}$$

where the symbol $\Delta \rightarrow \oint \dots dt$ implies the cumulative change of variables obtained by path integration of the individual terms in Eq. (14) over the field period. Since the internal energy U is an extensive thermodynamic variable, $\Delta U = 0$ holds in the steady state when the states α, state energies E_α and probabilities P_α in Eq. (12) become periodic functions of time. Therefore, the steady state behaviour implies:

$$\Delta W = -\Delta Q^e \tag{31}$$

Fig. 4(b) shows that Eq. (31) holds in the steady state once the initial transient field periods died out.

Similarly, integrating Eq. (16) over the field cycle gives:

$$T\Delta S = \Delta Q^e + \Delta Q^p \tag{32}$$

where we expressed the entropy changes accumulated over the field period through Eqs. (13) and (21). The total entropy is an extensive thermodynamic variable and thus $\Delta S = 0$ in the steady state, which leads to

$$\Delta Q^e = -\Delta Q^p \tag{33}$$

Thus the heat produced by the particles flows out of the system into the heat bath. Eq. (33) is validated in Fig. 4(c), which shows that in the steady state the relative difference between the entropies reduces to zero. Combining Eqs. (31) and (33) gives:

$$\Delta W = \Delta Q^p \tag{34}$$

which is the well known result stating that in the steady state the work performed over the field cycle, measurable by the hysteresis loop area, quantifies the heat produced by the MP system.

Similar argumentation applies to individual MPs within the chains. Integrating Eq. (27) over the field period and using (29) gives:

$$T\Delta S_i = \Delta Q_i^e + \Delta Q_i^p \tag{35}$$

which is analogous to Eq. (32) with the difference that it holds for a single particle i within the chain. The additive property of the total entropy change Eq. (17) over the individual transition paths suggests that the single particle total entropy can be seen as an extensive thermodynamic variable. Hence in the steady state we expect $\Delta S_i = 0$ and Eq. (35) turning to:

$$\Delta Q_i^e = -\Delta Q_i^p \tag{36}$$

Fig. 4(d) validates Eq. (36) in the steady state.

Finally, integrating Eq. (14) over a periodic field process, applying the fact that the internal energy is an extensive thermodynamic variable, and expressing the right hand side formulas as sums over the individual particles we obtain:

$$\sum_i \Delta W_i = -\sum_i \Delta Q_i^e \tag{37}$$

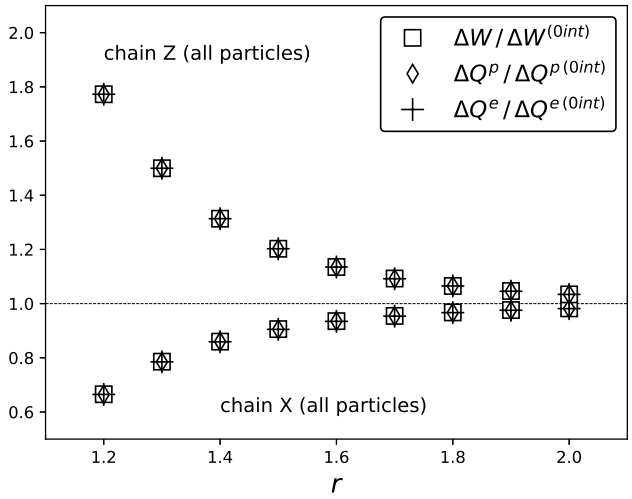

FIG. 5. Inter-particle distance dependence of the steady state work and entropy contributions over a field period validating Eqs. (31), (33), and (34), assuming 3-particle X and Z chains shown in Figs. 1. The simulation parameters were: $a = 11$ nm, $H_0 = 24$ kA/m, and $f = 300$ kHz.

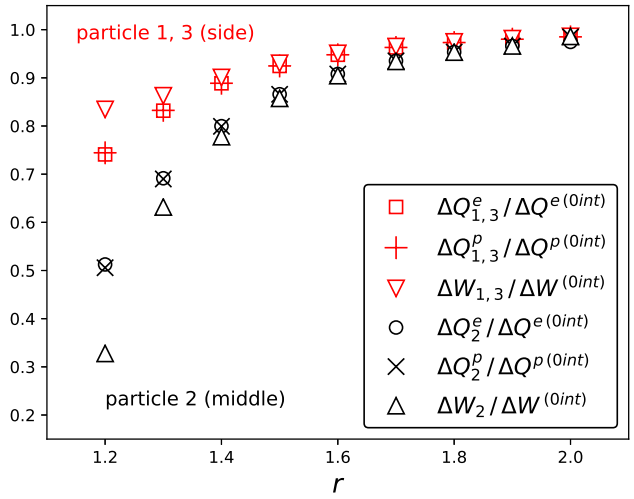

FIG. 6. Inter-particle distance dependence of the steady state individual particle work and entropy contributions over a field period validating Eq. (36) and demonstrating the inequality in Eq. (38). Data correspond to the 3-particle X chain shown in Figs. 1 and 2. By symmetry data for particle 1 and 3 is equivalent. The simulation parameters were: $a = 11$ nm, $H_0 = 24$ kA/m, and $f = 300$ kHz.

which, unfortunately, cannot be reduced to equivalent expressions for individual particles, i.e.:

$$\Delta W_i \neq -\Delta Q^e_i = \Delta Q^p_i \tag{38}$$

where the second equality follows from Eq. (36). Thus the work performed on a MP in a chain by the applied external field can no longer be used as a measure of heat. This is demonstrated in Fig. 4(e), which shows a finite difference between ΔW_i and $-\Delta Q^e_i$ even in the steady state. As discussed below, the difference between the single particle work and heat depends on the particle properties and the inter-particle interaction strength.

VI. RESULTS AND DISCUSSION

We have performed extensive testing of the concepts developed above for various kinds of chains with variable properties of MPs, field amplitudes and frequencies. As an example, Fig. 5 shows the normalised ΔW, ΔQ^e, and ΔQ^p calculated for 3-particle Z and X chains as a function of the distance between the neighbouring particles r. The normalisation was performed by the non-interacting particle case $\Delta W^{(0int)}$, $\Delta Q^{e(0int)}$ and $\Delta Q^{p(0int)}$, which can be evaluated based on the single-particle calculations and symmetry arguments [18]. All of the data for a given chain type overlap, in agreement with Eq. (34). The figure also shows that as the relative distance between the particles decreases, thereby enhancing the dipolar interaction strength, the produced heat increases for Z chains and decreases for X chains. This result is consistent with the previous findings [37], and can be attributed to the interactions effectively increasing/decreasing the effective energy barriers for Z/X chains.

Fig. 6 shows similar calculations but this time considering the individual particle behaviour in the 3-particle chain X. As confirmed by the data agreement, Eq. (36) always holds for any MP in the chain. However, the single-particle cyclic work ΔW_i no longer represents the heat ΔQ^p_i produced by MPs, as expected based on Eq. (38). As shown in the figure, the discrepancy between the work and heat increases with the decreasing inter-particle distance r due to the enhanced dipolar interaction strength. Similar discrepancy is observed for Z chains (not shown). Thus, unlike the area of the hysteresis loop of the entire chain, the area of the hysteresis sub-loops of individual particles (Fig. 2) cannot be associated with the heat production, and using explicit calculations based on Eqs. (24)-(26) and (29) becomes necessary.

The results of such calculations for chains of length varying from 1 to 6 particles are shown in Fig. 7. SAR refers to the so-called specific absorption rate, which is typically used to specify the heat power $\mathcal{P}$ (heat per unit time) produced by MPs subject to alternating magnetic fields, and when expressed for individual particles reads:

$$\mathrm{SAR}_i = \frac{\mathcal{P}_i}{V\rho} = \frac{f\Delta Q^p_i}{V\rho} \tag{39}$$

where f is the field frequency, and the product of volume and mass density, $V\rho$, is the particle mass. Eq. (39) is typically expressed through the hysteresis loop area, i.e. $\mathcal{P}_i = f\Delta W_i$, however, in view of Eq. (38) we base our definition directly on ΔQ^p_i.

Fig. 7(a) shows the computed normalised SAR_i corresponding to MPs across the chains X of variable lengths.

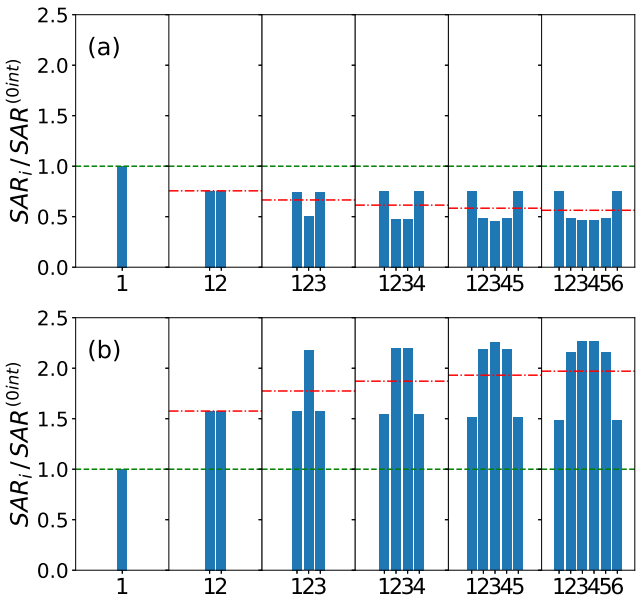

FIG. 7. Calculations of distributions of the individual particle SAR_i normalised by the non-interacting case $\mathrm{SAR}^{(0int)}$ (dashed line) across the X (a) and Z (b) chains of length increasing from 1 to 6 particles from left to right. The dash-dotted line is the average heat per particle. The simulation parameters were: $a = 11$ nm, $H_0 = 24$ kA/m, $r = 1.2a$, and $f = 300$ kHz.

The normalisation is with respect to $\mathrm{SAR}^{(0int)}$ of non-interacting MPs (dashed line). The dash-dotted line represents the average SAR computed from hysteresis loops of full chains divided by the number of MPs per chain. The figure shows that there is a substantial decrease of SAR across chains in comparison to the non-interacting case, which becomes more significant as the number of MPs per chain grows. The heating is most substantial for corner MPs, exceeding the average heat, whereas it becomes suppressed for inner MPs inside chains. Fig. 7(b) shows similar calculations for the Z chain configuration. In this case, SAR is significantly enhanced for inner MPs in chains, while the heating is smallest at the corner MPs.

The heat distributions correlate with the cumulative dipolar field effect across the chains, which is the weakest in the centre of X chains and strongest in the centre of Z chains. It is expected that in the long-chain limit $N \to \infty$ the dipolar field acting on MPs sufficiently far away from the edges of chains becomes asymptotically uniform. It is then reasonable to approximate the single-particle heat as $\Delta Q_i^p \approx \Delta Q^p / N = \Delta W / N$, where ΔQ^p is the cumulative heat produced by the entire chain, which according to Eq. (34) equals the work ΔW measurable by the area of the hysteresis loop corresponding to the chain.

VII. CONCLUSIONS

In summary, the developed thermodynamic framework allows to explicitly evaluate the entropy production and consequently the heat distributions in systems of interacting MPs. Although our study was based on MP chains, the framework can be naturally applied to MP clusters and aggregates if the underlying energy barriers can be identified. Our calculations in Fig. 7 suggest that the presence of dipolar interactions may contribute to significant heat distributions within MP assemblies. The heat distributions are expected to be even more pronounced in planar and three dimensional MP clusters due to the possibility of higher MP packing fractions enhancing the local dipolar effects. This could lead to considerable local heating produced inside cancer cells while the net temperature effect remains small, corroborating the earlier experimental findings [10, 11].

The developed formalism can be applied in other application settings such as, for example, in magnetic recording, which often relies on similar modelling techniques [38, 39], or for evaluating the entropy changes in MP systems for magnetic refrigeration [2]. It can also be applied naturally to study problems outside of particulate magnetism such as, for example, to model nanoscale friction [40] or biological systems [20].

We also note that the formalism developed in this work can be extended beyond the assumption of single-particle transitions applicable mostly to weakly interacting MP systems, once the network of transitions has been extended to include multi-particle switching events. However, this also requires generalising the notion of single particle heating to coherent particle switching events likely to occur across MP assemblies when dipolar interactions become significant.

VIII. ACKNOWLEDGEMENTS

P. T. acknowledges financial support from H2020 MSCA ITN project Solution No. 721642. D. S. acknowledges Xunta de Galicia for financial support under the I2C Plan. We also gratefully acknowledge support from an International Exchanges grant (IE160535) of the Royal Society, and from the Strategic Grouping in Materials (AeMAT grant No. ED431E2018/08).

[1] A. López-Ortega, M. Estrader, G. Salazar-Alvarez, A. G. Roca, and J. Nogués, Physics Reports **553**, 1 (2015).

[2] V. Franco, J. Blázquez, B. Ingale, and A. Conde, Annual Review of Materials Research **42**, 305 (2012).

[3] M. Angelakeris, Biochimica et Biophysica Acta **1861**, 1642 (2017).
[4] F. Wiekhorst, U. Steinhoff, D. Eberbeck, and L. Trahms, Pharmaceutical Research **29**, 1189 (2012).
[5] B. Gleich and J. Weizenecker, Nature **435**, 1214 (2005).
[6] E. A. Périgo, G. Hemery, O. Sandre, D. Ortega, E. Garaio, F. Plazaola, and F. J. Teran, Applied Physics Reviews **2**, 041302 (2015).
[7] M. L. Etheridge, K. R. Hurley, J. Zhang, S. Jeon, H. L. Ring, C. Hogan, C. L. Haynes, M. Garwood, and J. C. Bischof, TECHNOLOGY **02**, 214 (2014).
[8] N. A. Usov, O. N. Serebryakova, and V. P. Tarasov, Nanoscale Research Letters **12**, 489 (2017).
[9] O. Hovorka, Journal of Physics D: Applied Physics **50**, 044004 (2017).
[10] M. Creixell, A. C. Bohórquez, M. Torres-Lugo, and C. Rinaldi, ACS Nano **5**, 7124 (2011).
[11] L. Asin, M. Ibarra, A. Tres, and G. Goya, Pharmaceutical research **29**, 1319 (2012).
[12] J. T. Dias, M. Moros, P. del Pino, S. Rivera, V. Grazú, and J. M. de la Fuente, Angewandte Chemie International Edition **52**, 11526 (2013).
[13] A. Riedinger, P. Guardia, A. Curcio, M. A. Garcia, R. Cingolani, L. Manna, and T. Pellegrino, Nano Letters **13**, 2399 (2013).
[14] C. Munoz-Menendez, I. Conde-Leboran, D. Serantes, R. Chantrell, O. Chubykalo-Fesenko, and D. Baldomir, Soft Matter **12**, 8815 (2016).
[15] S. R. De Groot and P. Mazur, *Non-equilibrium thermodynamics* (Courier Corporation, 2013).
[16] R. E. Rosensweig, Journal of Magnetism and Magnetic Materials **252**, 370 (2002).
[17] S. Ruta, R. Chantrell, and O. Hovorka, Scientific Reports **5** (2015).
[18] G. Bertotti, *Hysteresis in magnetism: for physicists, materials scientists, and engineers* (Academic press, 1998).
[19] V. Basso, C. Beatrice, M. LoBue, P. Tiberto, and G. Bertotti, Physical Review B **61**, 1278 (2000).
[20] U. Seifert, Reports on Progress in Physics **75**, 126001 (2012).
[21] T. Tomé and M. J. de Oliveira, Phys. Rev. E **91**, 042140 (2015).
[22] C. Van den Broeck and M. Esposito, Physica A: Statistical Mechanics and its Applications **418**, 6 (2015).
[23] A. Aharoni, *Introduction to the Theory of Ferromagnetism* (Clarendon Press, 2000).
[24] W. Brown, Jr., IEEE Transactions on Magnetics **15**, 1196 (1979).
[25] H. Pfeiffer, physica status solidi (a) **118**, 295 (1990).
[26] O. Hovorka, J. Barker, G. Friedman, and R. W. Chantrell, Physical Review B **89** (2014).
[27] O. Laslett, S. Ruta, J. Barker, R. W. Chantrell, G. Friedman, and O. Hovorka, Applied Physics Letters **106**, 012407 (2015).
[28] J. Schnakenberg, Rev. Mod. Phys. **48**, 571 (1976).
[29] W. H. Press, S. A. Teukolsky, W. Vetterling, and B. P. Flannery, *Numerical recipes in C* (Cambridge University Press, 1992).
[30] W. F. Brown, Phys. Rev. **130**, 1677 (1963).
[31] J. L. García-Palacios and F. J. Lázaro, Phys. Rev. B **58**, 14937 (1998).
[32] W. Wernsdorfer, E. B. Orozco, K. Hasselbach, A. Benoit, B. Barbara, N. Demoncy, A. Loiseau, H. Pascard, and D. Mailly, Phys. Rev. Lett. **78**, 1791 (1997).
[33] S. K. Piotrowski, M. F. Matty, and S. A. Majetich, IEEE Transactions on Magnetics **50**, 1 (2014).
[34] A. Hevroni, B. Tsukerman, and G. Markovich, Physical Review B **92**, 224423 (2015).
[35] H. B. Callen, *Thermodynamics and an Introduction to Thermostatistics* (American Association of Physics Teachers, 1998).
[36] Y.-C. Cheng, *Macroscopic and Statistical Thermodynamics* (World Scientific Publishing Company, 2006).
[37] D. Serantes, K. Simeonidis, M. Angelakeris, O. Chubykalo-Fesenko, M. Marciello, M. del Puerto Morales, D. Baldomir, and C. Martinez-Boubeta, The Journal of Physical Chemistry C **118**, 5927 (2014).
[38] O. Hovorka, R. F. L. Evans, R. W. Chantrell, and A. Berger, Applied Physics Letters **97**, 062504 (2010).
[39] O. Hovorka, J. Pressesky, G. Ju, A. Berger, and R. W. Chantrell, Applied Physics Letters **101**, 182405 (2012).
[40] P. C. Torche, T. Polcar, and O. Hovorka, Physical Review B **100**, 125431 (2019).